Pergamon

Int. J. Heat Mass Transfer. Vol. 40, No. 10, pp. 2293–2305, 1997

0017–9310/97 $17.00+0.00

PII: S0017–9310(96)00304–3

Simulation and measurement of a vertical Bridgman growth system for β-NiAl crystal

H. OUYANG† and W. SHYY‡

Department of Aerospace Engineering, Mechanics and Engineering Science, University of Florida, Gainesville, FL 32611, U.S.A.

and

V. I. LEVIT and M. J. KAUFMAN

Department of Materials Science and Engineering, University of Florida, Gainesville, FL 32611, U.S.A.

(*Received* 8 *July* 1996 *and in final form* 21 *August* 1996)

Abstract—A coordinated theoretical and experimental study of the temperature distribution inside a customized vertical Bridgman system for growing β-NiAl crystal has been conducted. The theoretical model accounts for the combined effects of phase change dynamics, the coupled heat transfer processes of conduction, convection and radiation, variable material properties, and complex geometry pertaining to the system. Comparisons between numerical predictions and experimental measurements show satisfactory agreement. The accuracy of the melting temperature of NiAl with stoichiometric composition, along with important processing parameters such as interface curvatures and temperature gradients across the interface, have been discussed in detail. Also assessed are possibilities of improving the solidification process, including coating the ampoule outer wall with a material of high radiative emissivity or decreasing the ampoule wall thickness. © 1997 Elsevier Science Ltd. All rights reserved.

1. INTRODUCTION

The physical and mechanical properties of nickel aluminum (NiAl) depend strongly on both composition and temperature [1–6]. At stoichiometric composition (50 at.% Ni, 50 at.% Al), NiAl has its lowest yield strength and highest ductility, while transition temperature from brittle to ductile behavior (BDTT) is at a minimum [2]. Impurity content and deviations from stoichiometry can significantly change these properties. For example, it has been found that single crystal NiAl with improved purity [1] or with small (< 1%) additions of iron, gallium or molybdenum [5] yields substantial increase of ductility at room temperature. As far as the temperature effect is concerned, it has been widely recognized that NiAl, like most other intermetallics, has the drawbacks of poor ductility at room temperature and low strength at elevated temperature, despite its many other superior advantages such as low density, high thermal conductivity and high melting temperature [2, 5–6]. These problems need to be resolved before NiAl will be useful in structural applications as a high temperature material.

The present work represents part of a systematic effort conducted with the goal of understanding the behavior of NiAl from two aspects, i.e. the influence of alloying and processing on the structure and properties of NiAl. Alloying mostly deals with the procedure of additions of certain elements or other precipitates to the single crystal for the purpose of property enhancement. Processing, on the other hand, is mainly concerned with the change of thermal conditions by factors such as selection of ampoule materials, setup of heating and cooling temperatures, and variation of growth speed. The current study is focused on the processing conditions in a vertical Bridgman system for growing single crystal β-NiAl, having a composition of 50 at.% Ni, 50 at.% Al, with a B2 (CsCl) crystal structure. The information obtained facilitates a better understanding of the various processing parameters, which, in turn, offer guidance to adjust the processing environment for enhancing crystal quality and composition control.

In the present study, initially, the raw material of NiAl is vacuum induction melted and chill cast into a rod with a desired size. The rod is then removed from the chill mold, placed in a high density refractory (e.g. alumina) ampoule, which is situated on top of a water cooled ram (e.g. copper), remelted and then directionally solidified by slowly withdrawing the ampoule/ram assembly from the hot zone. In most cases, a single crystal seed is placed between the chill and the feedstock in order to preselect the orientation of the single crystal NiAl. Figure 1 (a) shows the schematic of such a Bridgman system. Several physical mech-

† Current Address: Atchison Casting Corporation, Quaker Alloy Division, Myerstown, PA17067, U.S.A.

‡ Author to whom correspondence should be addressed.

NOMENCLATURE

C_p	specific heat	$T1$	coolant temperature
g	gravitational acceleration	$T4$	heater temperature
H	ampoule position within the furnace	TC1, TC2	thermocouple reading
		TC3, TC4	thermocouple reading
ΔH	latent heat	u	radial velocity component
k	thermal conductivity	w	axial velocity component
P	static pressure	z	axial coordinate
R	radial position from the reference point of the ampoule (see Fig. 1)	Z	axial position from the reference point of the ampoule (see Fig. 1).
r	radial coordinate		
Su, Sw	source terms in the momentum equations	Greek symbols	
		β	thermal expansion coefficient
T	temperature	μ	viscosity
T_{ref}	reference temperature	ϱ	density.

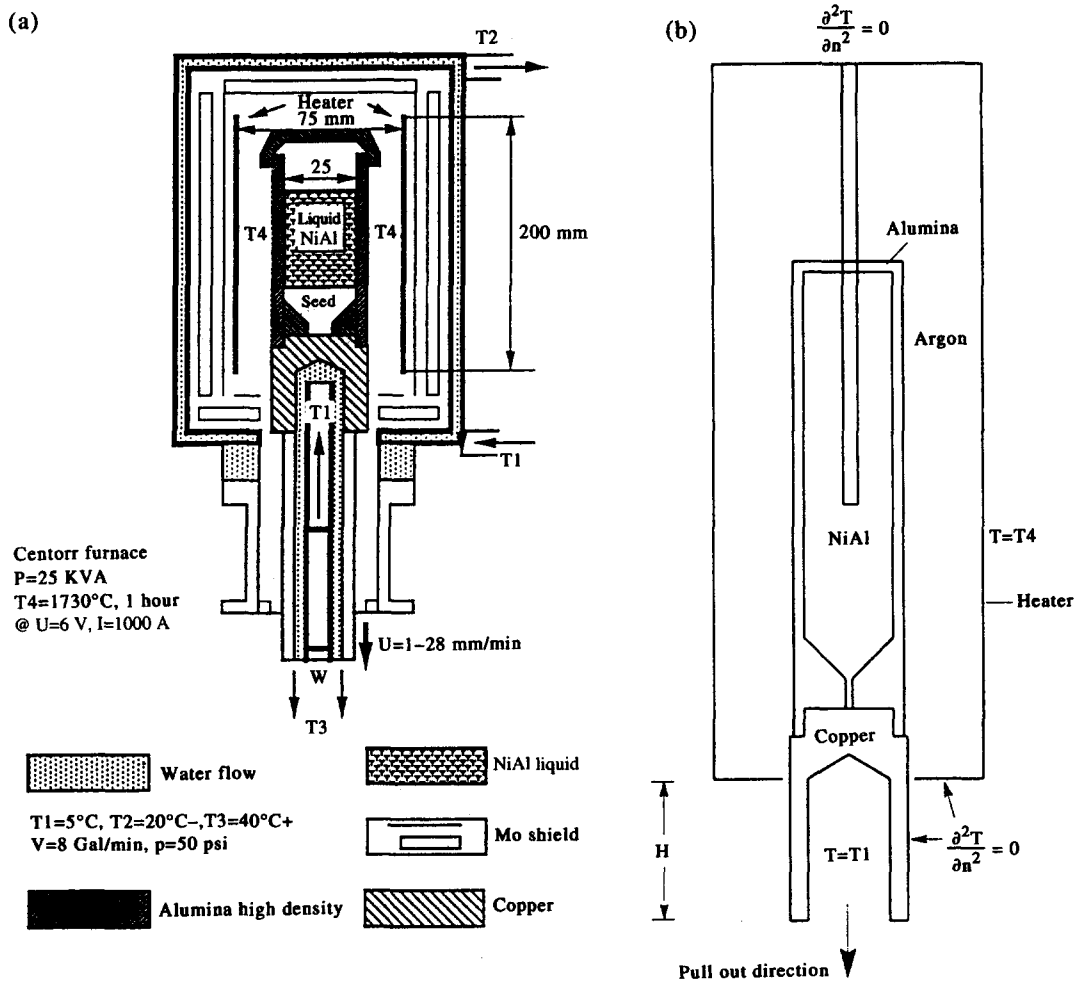

Fig. 1. Vertical Bridgman growth system for β-NiAl crystal: (a) schematic of actual design; (b) layout and boundary conditions extracted from (a) for numerical simulation, where H measures the ampoule position with respect to the heater baseline as it is pulled out, $T4$ = 1800°C and $T1$ = 10°C.

anisms can be identified in this system and are of key importance to the processing conditions. These include the phase change dynamics between the NiAl melt/solid interface, heat conduction across the ampoule wall and the copper ram, convection in the melt and in the encapsulated argon gas, and radiation between the outer ampoule wall and the heater, which is held at T4, surrounding the ampoule.

We have developed a numerical model to simulate the thermal and solidification characteristics of this system, accounting for the coupled heat transfer processes, complex geometry, as well as variable material properties [7, 8]. To validate this model, experimental measurements of temperature profiles at designated locations in a vertical Bridgman growth system for β-NiAl single crystal have been made and compared with the predictions. To help optimize the thermal conditions for growing single crystal β-NiAl with desired properties, parametric variations have also been considered in numerical simulations. Furthermore, the exact melting temperature of NiAl does not seem to have been ascertained; combining the computational and experimental information, the correct value of the melting temperature is assessed.

2. EXPERIMENTAL PROCEDURE

2.1. *System set-up*

Figure 1(a) shows the schematic of the current vertical Bridgman growth system, which is axisymmetric. Compared to the previous work [7, 8], in this study, the ampoule inner diameter has been increased from 25 to 29 mm diameter to grow a larger crystal. The feedstock of NiAl was prepared by vacuum induction melting and chill casting into a 28 mm diameter rod, with a 5 mm diameter hole in the center to allow for installation of a thermocouple.

Four Type C tungsten–rhenium thermocouples with 3 mm diameter were installed for measuring the temperature profiles and furnace hot zone temperature during the crystal growth process. Figure 2 shows the detailed arrangement of these thermocouples. Thermocouple 1 (TC1) was positioned along the centerline of the NiAl feedstock. To protect this thermocouple from corrosion and contaminating the crystal during the melting process, it was enclosed by an alumina tube using a 3 mm inner diameter and 5 mm outer diameter and a tip length of 6.5 mm. This arrangement also allows thermocouple 1 to translate vertically along the NiAl centerline. Thermocouple 2 (TC2) was positioned along the outer ampoule wall and was also allowed to translate vertically. In addition, thermocouples 3 and 4 (TC3 and TC4) were fixed horizontally at about one-half height of the heater. They were used to help monitor the thermal condition in the furnace hot zone during the entire crystal growth process. All thermocouples were calibrated before the installation. However, it has to be mentioned that the confidence limit for type C thermal couple is 1%.

The relative positions of the various components in the system were measured with respect to the baseline of the sealing frame as shown in Fig. 1(a) and Fig. 2. While the relative positions of the ampoule and thermocouples are taken with respect to the bottom of the heater, shown in Fig. 2 by the horizontal radial axis R. The ampoule position is denoted by H, which is initially set as 43 mm. As the ampoule is pulled down, this number increases. h denotes the tip positions of thermocouple 1 or 2. Because of the interior complexity and small scale of the current system, the measurement of positions is estimated to have a confidence limit of ± 1 mm.

2.2. *Temperature measurement*

In the course of making temperature measurements, the system was first heated for about 3.5 h until TC3 and TC4 reached 1740°C. Then the system was held for another 30–45 min to allow the NiAl feedstock to melt. Next, the ampoule/ram assembly was withdrawn from the furnace and stopped at designated positions to allow TC1 and TC2 to take measurements at different positions, as described next.

After the NiAl feedstock was melted, the alumina tube with thermocouple TC1 was moved down through the melt until it stopped and touched the melt/solid interface. Hence, the interface position for the initial ampoule position of $h = 43$ mm could be located. Thereafter, the alumina tube remained at this position, while TC1 was allowed to translate vertically. Once temperature readings from TC1 and TC2 were stable, TC1 and TC2 were moved to a new height and the corresponding temperatures obtained. For the convenience of measurement, TC1 and TC2 were always moved in tandem. After measurements at various h positions were made, the ampoule/ram assembly was withdrawn and stopped at a designated new ampoule position, e.g. $H = 59$ mm, where temperatures were once again measured. This process was repeated until the desired number of ampoule positions were measured. In the present work, temperature profiles, along the NiAl centerline and the ampoule outer wall, were measured for a total of six ampoule positions, $H = 43$, 59, 67, 77, 87 and 97 mm. Table 1 and Fig. 3 summarize the data collected. The number of data points collected decreases as the ampoule is pulled out (H increases), since the thermocouples traverse a smaller length. In addition, the interface position was only obtained for the first ampoule position of $H = 43$ mm. The measured interface position, with respect to the bottom line of the heater (R axis), is 75 mm. This number is checked once again after the experiment when the solidified NiAl ingot was broken and the position of the tip trace of the alumina tube was measured. The result showed that the confidence limit for the interface measurement is about ± 2 mm. During the entire experimental process, a stable furnace temperature of 1740 ± 1°C was maintained by manually adjusting the input power about a baseline value of 7 kW.

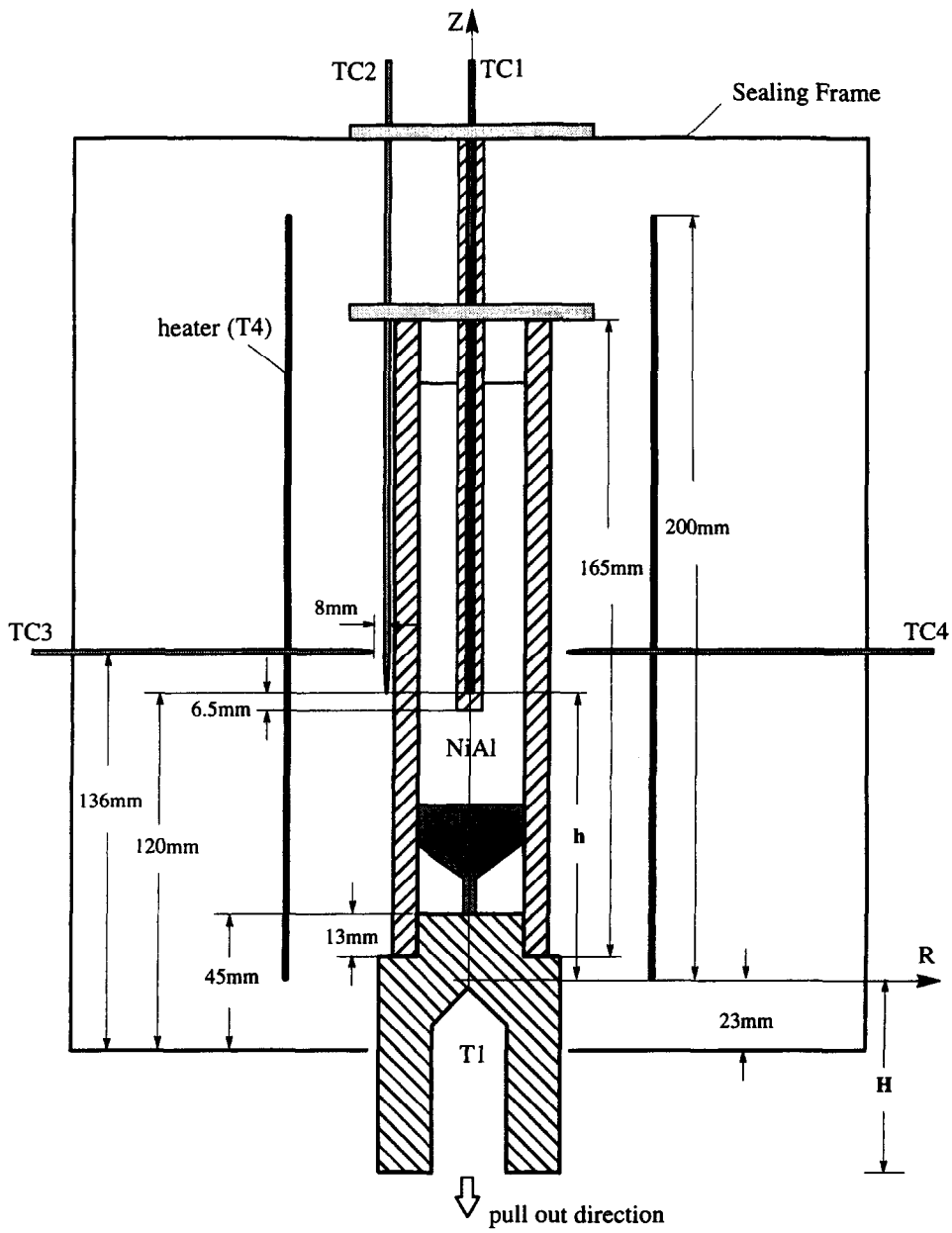

Fig. 2. Setup of thermocouples for the experimental measurement of temperature.

2.3. *Experimental observations*

From Table 1 and Fig. 3, it can be seen that the temperature measured along the outer ampoule wall can be up to 1796°C, which is higher than the value of 1740°C measured by TC3/TC4. Even at the same height, the temperature value at the ampoule outer wall is about 40°C higher than that of TC3/TC4, although their horizontal gap is only about 8 mm as shown in Fig. 2. It is also observed that, when TC3 or TC4 touches the ampoule outer wall, it yields the same temperature as that is measured by TC2. However, when TC3 or TC4 is pulled horizontally away from the ampoule, its temperature reading drops significantly. The cause of this substantial discrepancy of temperature is unclear at present, but might be explained by the effect of radiation. Figure 4 shows this situation more clearly in a top view of the system. It can be seen that the tips of TC3 and TC4 both face directly to the ampoule wall instead of the heater, hence they receive less radiation from the heater than TC2, resulting in a lower temperature. In addition, it is also observed from Fig. 3 that the temperature gradient in the axial direction is higher at the lower portion of the ampoule than at the higher portion of the ampoule. As the

Table 1. Temperature vs thermal couple positions (h) for different ampoule positions (H)

H [mm]	Thermocouple 1 (located along the NiAl centerline)						
43	h [mm]	82	88	98	108	118	
	T [°C]	1737	1752	1766	1774	1778	
59	h [mm]	63	78	88	98	108	
	T [°C]	1734	1762	1774	1779	1782	
67	h [mm]	56	68	83	93	103	
	T [°C]	1733	1758	1773	1782	1784	
77	h [mm]	54	58	68	78	88	
	T [°C]	1752	1758	1772	1780	1785	
87	h [mm]	54	63	73	83		
	T [°C]	1762	1773	1780	1780		
97	h [mm]	54	58	68	73		
	T [°C]	1767	1770	1778	1780		

H [mm]	Thermocouple 2 (located along the ampoule outer wall)						
43	h [mm]	82	88	98	108	118	
	T [°C]	1780	1786	1791	1795	1796	
59	h [mm]	54	63	78	88	98	108
	T [°C]	1761	1773	1787	1791	1793	1793
67	h [mm]	56	68	83	93	103	
	T [°C]	1773	1783	1792	1794	1795	
77	h [mm]	54	58	68	78	88	
	T [°C]	1779	1782	1788	1793	1794	
87	h [mm]	54	63	73	83		
	T [°C]	1779	1787	1790	1793		
97	h [mm]	54	58	68	73	83	93
	T [°C]	1782	1784	1789	1790	1793	1794

ampoule is pulled out (H increases), temperature profiles along both the NiAl centerline and the ampoule outer wall become more unified.

3. COMPARISON WITH NUMERICAL SIMULATION

3.1. *Modeling considerations*

We have mentioned before that, in the vertical Bridgman system, there exists complicated physical phenomena of phase change, conduction, convection and radiation heat transfer, variable material properties and complex geometry. Previously, we have developed a comprehensive numerical model that could take into account all these factors [7, 8]. In the present effort, we compare the modeling predictions by this method with experimental results. In order to accomplish this, several modifications to the model have been made to meet the specific conditions adopted in the current experiment.

First, as explained previously, the geometry of the experimental system had to be changed to accommodate the thermocouples. The inserted alumina tube along the NiAl centerline has a diameter about one sixth of the ampoule inner diameter of 29 mm. Hence, the interference caused by the alumina tube had to be considered.

The second change is in boundary condition specification. In the previous study [7, 8], we used

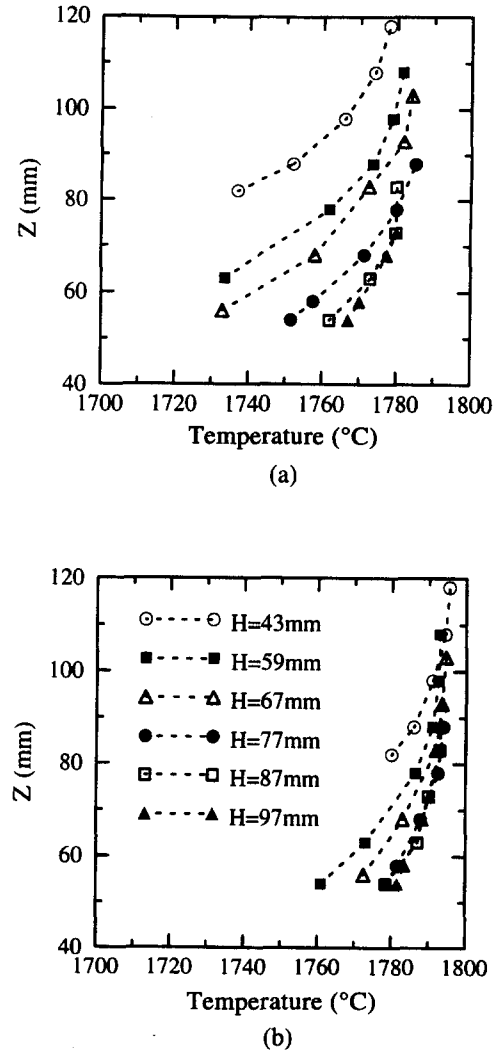

Fig. 3. Experimental result of temperature profiles along: (a) the NiAl centerline; and (b) the ampoule outer wall for different ampoule position H.

T4 = 1740°C as the heater boundary condition, which is actually the temperature measured by TC3/TC4. From the aforementioned experimental set-up, the heater temperature cannot be directly measured. However, the highest temperature along the ampoule outer wall was measured by TC2 to be 1796°C. Therefore, the heater temperature T4 can be estimated to be 1800°C, based upon previous numerical results which showed a 3–5°C difference in temperature between the heater and the alumina wall. The cooling water temperature ranged from 5 to 10°C (city water). When the cooling water reaches the copper ram, it will be warmed up somewhat, so we use the upper limit of T1 = 10°C as the cooling boundary condition. For the rest of the boundaries in the furnace, temperature boundary conditions are difficult to give directly. Estimation can be made, though, according to the experimental characteristics. We have mentioned that, during the entire crystal growth process, the furnace hot

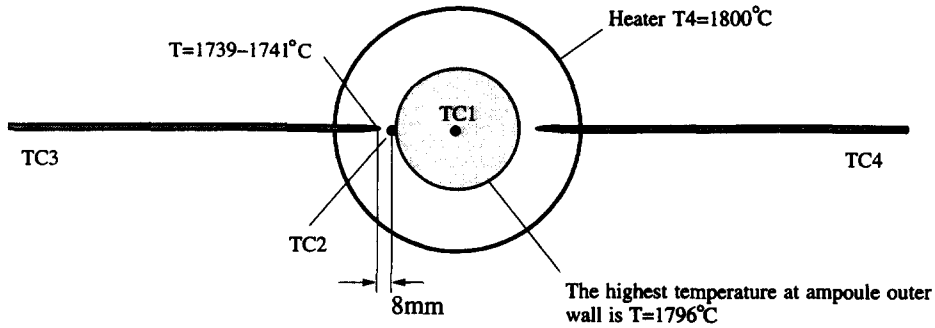

Fig. 4. The top view of the arrangement of thermocouples in the NiAl furnace.

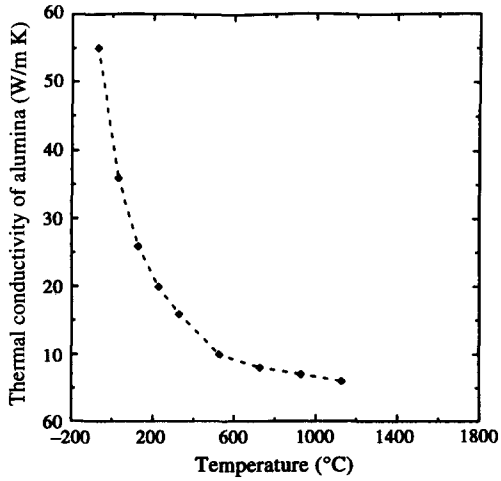

Fig. 5. Dependency of thermal conductivity of alumina on temperature.

zone temperature was maintained at a stable value of 1740°C by manually adjusting the stable power input. In other words, a constant heat flux condition is imposed for the remaining furnace boundaries, i.e. $\partial T^2/\partial n^2 = 0$.

The third consideration is the accurate specification of the material properties as functions of temperature. This is a very important factor in obtaining accurate numerical results. As shown in Table 1 and Fig. 3, the majority of the alumina ampoule is exposed to a temperature range above 1700°C, which exceeds the upper threshold (1127°C) of conductivity as a function of temperature, $k(T)$, shown in Fig. 5 [9]. Therefore, in this modeling effort, conductivity of alumina above $T = 1127$°C has been estimated by extrapolation of the gradient of $k(T)$ at $T = 1127$°C.

3.2. *Modeling result*

A similar set-up of the computational domain as adopted in ref. [8] is applied here, except that the alumina tube has been considered in this case, shown in Fig. 1(b). The governing equations, in conjunction with the enthalpy formulation for phase change, Boussinesq approximation for buoyancy effect and variable material properties, are given as:

(i) Continuity equation

$$\frac{\partial}{\partial r}(\varrho ru) + \frac{\partial}{\partial z}(\varrho rw) = 0. \tag{1}$$

(ii) Momentum equation

r-momentum

$$\frac{\partial}{\partial t}(\varrho ru) + \frac{\partial}{\partial r}(\varrho ruu) + \frac{\partial}{\partial z}(\varrho rwu) = -r\frac{\partial P}{\partial r} + \left\{\frac{\partial}{\partial r}\left(\mu r\frac{\partial u}{\partial r}\right) + \frac{\partial}{\partial z}\left(\mu r\frac{\partial u}{\partial z}\right)\right\} - \mu\frac{u}{r} + Su \tag{2}$$

z-momentum

$$\frac{\partial}{\partial t}(\varrho rw) + \frac{\partial}{\partial r}(\varrho ruw) + \frac{\partial}{\partial z}(\varrho rww) = -r\frac{\partial P}{\partial z} + \left\{\frac{\partial}{\partial r}\left(\mu r\frac{\partial w}{\partial r}\right) + \frac{\partial}{\partial z}\left(\mu r\frac{\partial w}{\partial z}\right)\right\} + \varrho rg\beta(T - T_{\text{ref}}) + Sw. \tag{3}$$

(iii) Energy equation

$$\varrho C_p\left\{\frac{\partial}{\partial t}(rT) + \frac{\partial}{\partial r}(ruT) + \frac{\partial}{\partial z}(rwT)\right\} = \frac{\partial}{\partial r}\left(kr\frac{\partial T}{\partial r}\right) + \frac{\partial}{\partial z}\left(kr\frac{\partial T}{\partial z}\right) - \Delta H\left\{\frac{\partial}{\partial t}(\varrho rf) + \frac{\partial}{\partial r}(\varrho ruf) + \frac{\partial}{\partial z}(\varrho rwf)\right\}. \tag{4}$$

The radiation heat transfer between the heater and the ampoule outer wall comes into play via boundary conditions. The detailed account of the formulation and the numerical solution of these equations can be found in refs. [7, 8]. As the pulling speed of the current crystal growth process is about 1–2 mm per h, steady-state computations are most likely sufficient.

3.2.1. *Comparison of temperature profiles.* Figures 6 and 7 show that the temperature distribution along the NiAl centerline and the ampoule outer wall obtained from the computational simulation matches

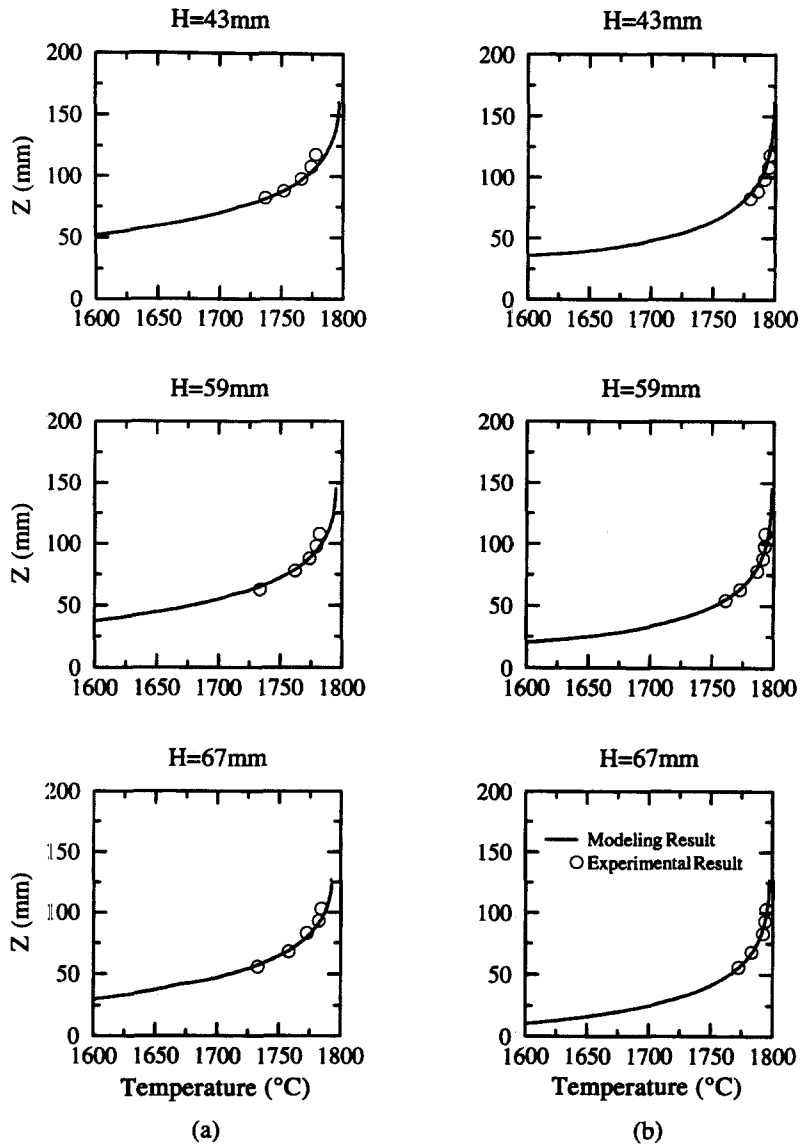

Fig. 6. Comparisons of temperature profiles along: (a) the NiAl centerline; and (b) the ampoule outer wall between the modeling result and the experimental data for the three higher ampoule positions of $H = 43$ mm, $H = 59$ mm and $H = 67$ mm.

the experimental measurements well overall. Satisfactory agreement is observed for all six ampoule positions, especially for the temperature along the outer alumina wall. This implies that both the simplified radiation model currently in use for computing the heat flux between the alumina outer wall and the heater, and the boundary condition of constant heat flux at the heater bottom are reasonable. Along the ampoule centerline, agreement between experimental data and computational results is good for the three higher ampoule positions of $H = 43$ mm, $H = 59$ mm and $H = 67$ mm, but worsens for the three lower ampoule positions. This trend is explained in more detail below.

Figure 8 shows the streamfunctions and isotherm distributions for two selected ampoule positions, one at a higher location ($H = 43$ mm) and the other at a lower location ($H = 87$ mm). For the higher ampoule position, Fig. 8(a) shows that the ampoule base region is contained inside the furnace hot zone. Since the treatment of radiation heat transfer and boundary conditions appear reasonable there shown by Fig. 6(b) and Fig. 7(b), the computed thermal distribution of this region is also accurate. Accordingly, the predicted temperature profile along the NiAl centerline matches very well with experimental results. At the lower ampoule position, Fig. 8(b) shows clearly that the ampoule base region has been pulled out of the furnace hot zone. In this case, the boundary condition at the outer wall of this region is still specified as a constant heat flux, which is no longer accurate. Furthermore, as the thermal distribution inside the

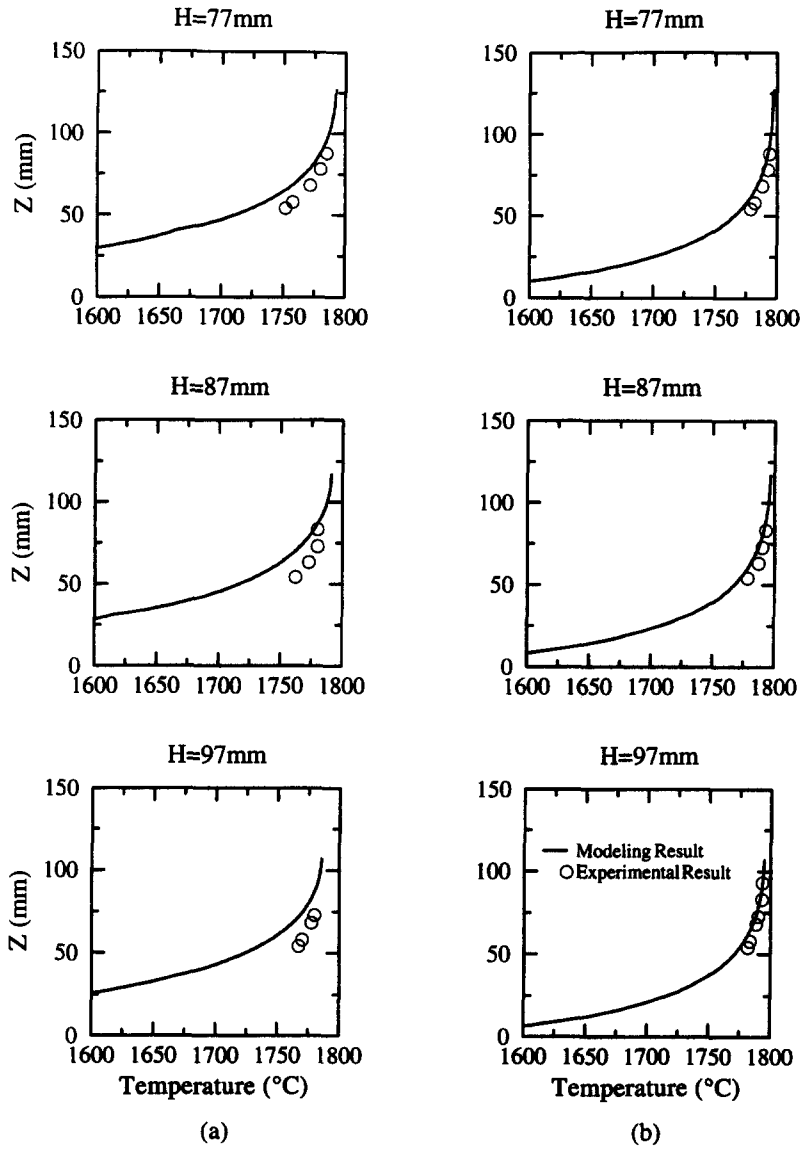

Fig. 7. Comparisons of temperature profiles along: (a) the NiAl centerline; and (b) the ampoule outer wall between the modeling result and the experimental data for the three lower ampoule positions of $H = 77$ mm, $H = 87$ mm and $H = 97$ mm.

ampoule is very sensitive to the isotherm change near the ampoule base, it is not surprising to observe in Fig. 7 some deviations between numerical results and experimental data along the NiAl centerline. Improvement of the modeling accuracy can be obtained by specifying realistic boundary condition at the outer ampoule wall as it is pulled out of the furnace. The temperature distribution along the ampoule outer wall in the furnace hot zone, though, is not influenced by this effect.

3.2.2. *Melting temperature of β-NiAl.* The melting temperature of NiAl at stoichiometric composition is reported in the literature as *Tmelt* = 1638°C [2, 3]. However, the accuracy of this value seems questionable. Since the pulling speed of the ampoule is slow and the convective strength within the melt is rather weak, solutions obtained with the steady-state conduction analysis are quite close to the full simulation for the present case. Based on the experimental data and conduction analysis, we are able to make a direct evaluation of the melting temperature of β-NiAl and compare it with the value adopted in the literature. The established melting temperature is also consistent with the solutions obtained by including the convective effect.

For the ampoule position of $H = 43$ mm, we measured the interface position by moving the alumina tube through the NiAl melt until it touched the solid/melt interface, which was found to be $h_{interf} = 75$ mm. It is noted that, since the tip of TC1 is separated from the interface by the closed end of the alumina tube (with a thickness of 6.5 mm shown in Fig. 2),

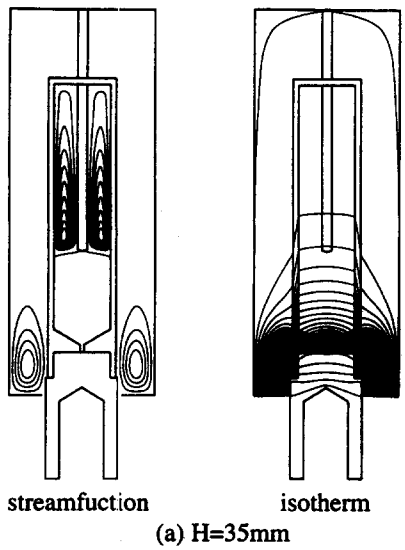

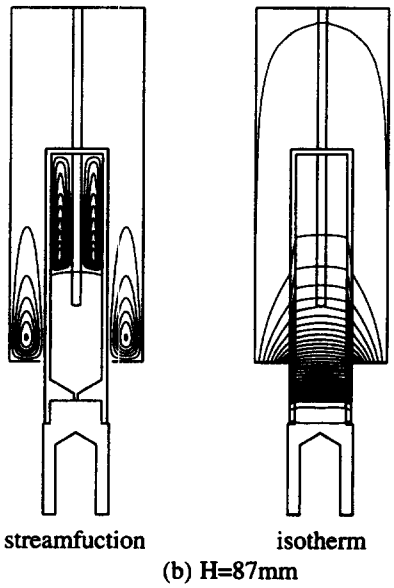

Fig. 8. Solution characteristics of NiAl furnace for selected ampoule positions of: (a) $H = 43$ mm; and (b) $H = 87$ mm.

the temperature reading of TC1 is not the melt/solid interface temperature. However, the detailed temperature profile along the entire ampoule centerline can be obtained from our numerical results. Combining these two results, the interface temperature of NiAl can be determined by interpolation, as shown in Fig. 9, yielding $T_{interf} = 1716°C$. This result is surprising, as this value is at least 70°C higher than the melting temperature of NiAl widely reported in the literature. Walston and Darolia [10] have also reported recently an observation of NiAl melting temperature as high as 1682°C. Although T_{melt} could not be determined directly in this study, the above estimation does seem to have its merit. Since the current numerical model correlates well with the experimental

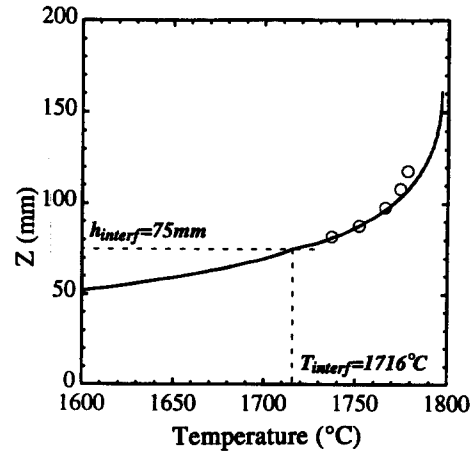

Fig. 9. The estimation of melt/solid interface temperature of β-NiAl.

data, the temperature profile we used for interpolating the interface temperature is likely to be accurate. It is noted that type C thermocouples have a confidence limit up to 1%, and hence can possibly result in about 18°C uncertainty in the present temperature measurement. The confidence limit of the solid/melt interface measurement is ± 2 mm. Considering all possible errors that might effect the measurements of temperature and interface position, the melting temperature we obtained for the NiAl sample at stoichiometric composition is still noticeably higher than 1638°C reported in the literature.

4. ASSESSMENT OF PROCESSING CONDITIONS VIA NUMERICAL MODELING

β-NiAl with high purity and improved mechanical property of high tensile elongation at room temperature has been produced routinely with the current design of the vertical Bridgman system [1]. Therefore, it is valuable to describe the detailed characteristics of the processing conditions that are suitable for growing high quality single crystal NiAl. Furthermore, based on the numerical simulation, we will also provide suggestions to improve design of the furnace components.

4.1. *Simulation of actual vertical Bridgman growth system*

Based on the satisfactory comparison between experimental and numerical results obtained for the case with thermocouples, we now turn our attention to the actual growth process without inserting the alumina tube. Figure 10 shows the solution characteristics of the stream function and isotherm at different ampoule positions. The convective fields in the melt are of very similar patterns at all ampoule positions, and the maximum velocity varies little. The convective strength in the encapsulated argon gas change more noticeably, but the maximum velocity there is at least one or two orders of magnitude smaller

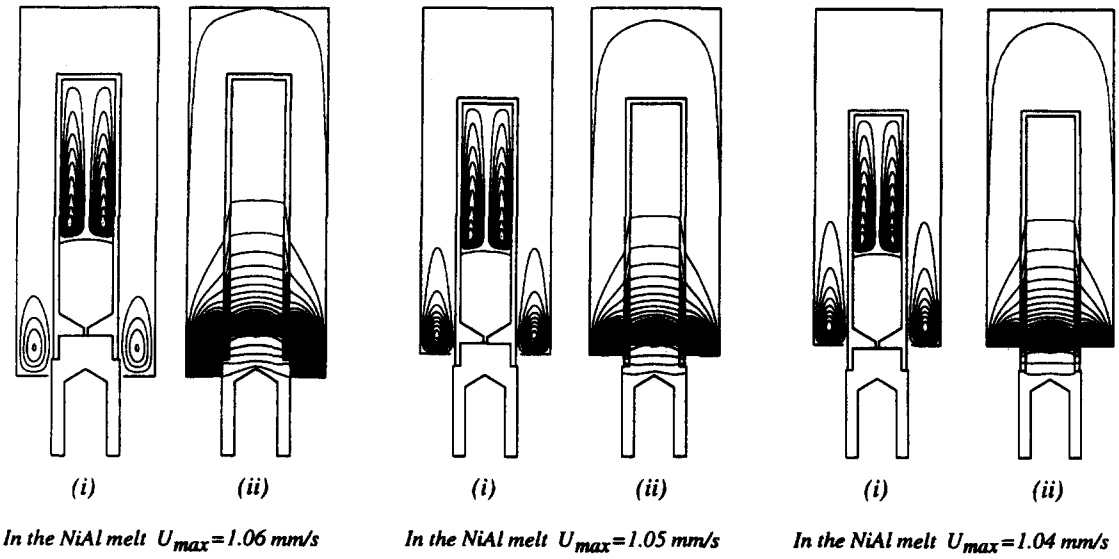

Fig. 10. Solution characteristics of (i) streamfunctions and (ii) isotherm in an actual vertical Bridgman growth system for NiAl crystal for different ampoule positions: (a) $H = 43$ mm; (b) $H = 59$ mm; and (c) $H = 67$ mm.

than that in the melt due to the higher Grashof number. As already discussed, the convective effects in the current crystal growth system are not strong. This is a desirable condition, for otherwise isotherms can be greatly distorted by convection which will cause nonuniform thermal gradients across the interface.

It has been recognized in the literature that, for crystal growth from the melt in the vertical Bridgman growth system, a slightly convex (toward the melt) liquid–solid interface can help prevent spontaneous nucleation at the ampoule wall. In addition, high temperature gradients across the interface and uniform distributions of thermal conditions along the interface are desirable for obtaining high purity crystals [11–13]. In the following, these aspects are further discussed.

Figure 11 shows the interface shape and the vertical temperature gradient across the interface at different ampoule positions. Due to the similar convective patterns, the interface shapes and temperature gradients obtained at ampoule positions are also close to each other. The difference between the centerline and inner ampoule wall locations is about 2 mm, and the gradients are all maintained within the range of 3.16–3.35°C mm^{-1}. Because of the convective effect in the melt, the temperature gradient at the interface centerline is about 5% higher than that at the inner ampoule wall. Figure 12 explains this situation more clearly, in which the interface characteristics with and without convection are compared. It is observed that convection causes the interface position to be moved up about 0.5%, which is quite small. However, it causes the temperature gradient across the interface to vary more noticeably (5%) along the interface, as shown in Fig. 12(b).

4.2. *Suggestions for design improvement*

In this section, we will vary design parameters with the goal of improving processing conditions in the vertical Bridgman growth system. Since convection has been found to be insignificant to affect the isotherm distributions within the melt in the present set-up, it is not included in order to save computational time. Parameters such as the ampoule emissivity, the geometry of the ampoule base, the thermal conductivity of the ram, and the ampoule wall thickness have been adjusted and their influence on the interface curvature and temperature gradient are compared. In the following, possible modification that might lead to the improvement of the interface conditions are listed.

- Case 1: the original design will be treated as the base case;
- Case 2: increase the emissivity of the ampoule outer wall from 0.8 to 1.0. This can be achieved in reality by, for example, coating the alumina ampoule outer wall with high emissivity and high melting temperature materials;
- Case 3: decrease the ampoule base angle from 120 to 100 degrees, as shown in Fig. 2;
- Case 4: use a higher thermal conductivity material for the chill ram. For example, replace copper by silver;
- Case 5: decrease the ampoule outer diameter by 2 mm.

Figure 13 shows the interface characteristics resulting from the variations of these parameters. It is observed that most of these variations can lead to certain increases of the temperature gradient across

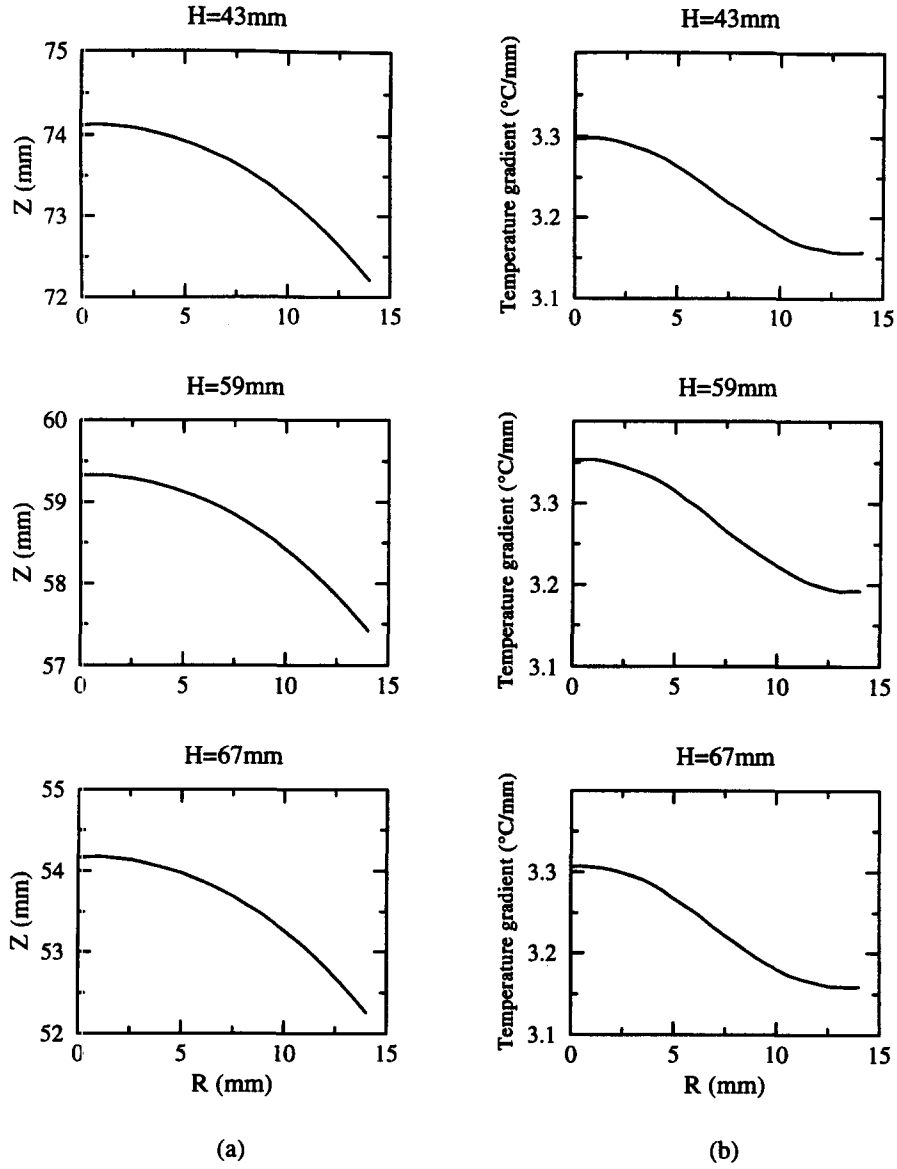

Fig. 11. (a) Interface characteristics; and (b) vertical temperature gradient across the interface for three ampoule positions of $H = 43$ mm, $H = 59$ mm and $H = 67$ mm.

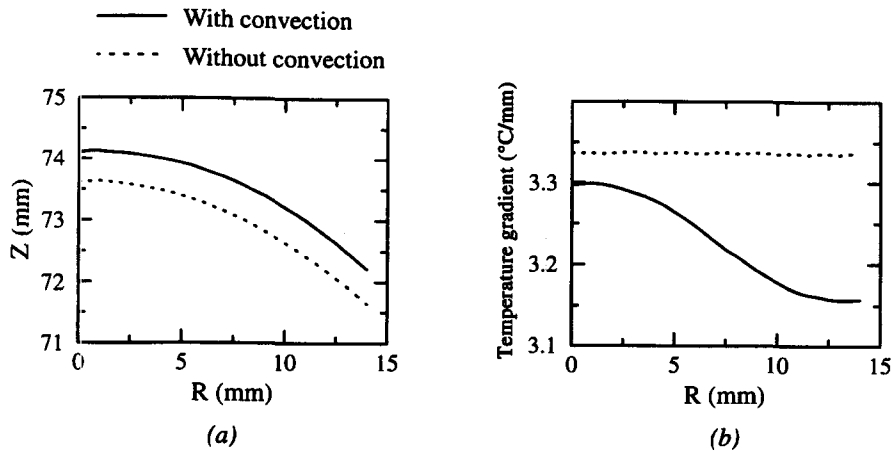

Fig. 12. Comparison of: (a) interface characteristics; and (b) temperature gradient across the interface between solutions with convection and without convection effects for the ampoule position of $H = 43$ mm.

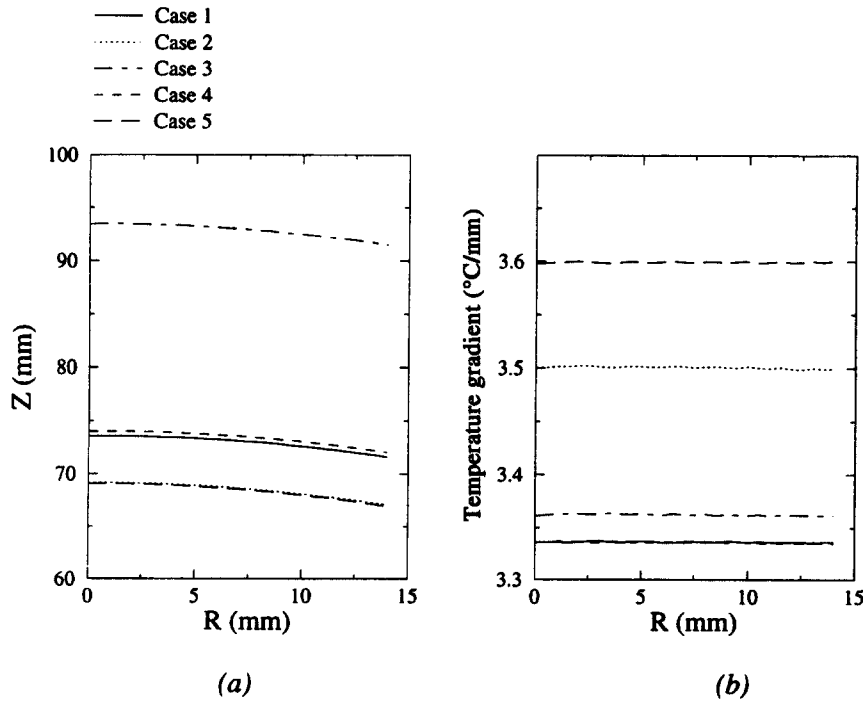

Fig. 13. Effects of variations in processing parameters on the interface characteristics by solutions without convection: (a) interface position; and (b) temperature gradient across the interface.

the solid/melt interface, which is desirable. In particular, for Cases 2 and 5, i.e. the increase of emissivity of the ampoule outer wall and the decrease of the ampoule thickness, the increase of the temperature gradient is more prominent. However, the change of the ram material to one with a higher conductivity (Case 4) seems not to influence the interface conditions much. It is interesting to observe that the interface curvature seems to be insensitive to these parametric variations. The locations of the interface, though, become lowered for Cases 2 and 5, higher for Case 3, and nearly unchanged for Case 4. It is desirable to further explore these factors by inspecting the quality of the crystal growth with these design modifications.

There are also other possible variations in furnace design that can potentially improve the processing condition near the interface. For example, it is obvious that an increase in heater temperature (T4) or a decrease of the cooling temperature (T1) helps increase the temperature gradient inside the system. However, care needs to be taken here because of the convection effect. It is observed from Fig. 12 that convection tends to cause the nonuniform distribution of temperature gradient along the interface, which is undesirable. Thus, any variations that can lead to increased convection strength should be made carefully.

5. CONCLUSION

In this study, we have conducted a detailed analysis of thermal conditions in a vertical Bridgman growth system for the β-NiAl single crystal. In this system, there are strongly coupled effects of phase change, conduction, convection and radiation heat transfer, variable material properties as functions of temperature, and complex geometry and boundary conditions. Therefore, optimization of the processing conditions for crystal growth is a very challenging task. In this study, we have coordinated computational and experimental efforts to first validate our theoretical model, then offer insight into possible design improvements. For example, we have shown that coating the ampoule outer wall with a high emissivity material, or decreasing the ampoule wall thickness can be advantageous. We have also found that the melting temperature of β-NiAl is around 1716°C, which is about 70°C higher than that reported in the literature. Because the high melting temperature of NiAl is one of its strongest attributes, the accurate definition of the melting temperature is of great interest. This important aspect should be further investigated.

Acknowledgment—This work has been partially supported by the Air Force Office of Scientific Research (URI Grant F49620-93-0309) under the direction of Dr Charles H. Ward.

REFERENCES

1. Levit, V. I., Bul, I. A., Hu, J. and Kaufman, M. J., High tensile elongation of β-NiAl single crystals at 293 K. *Scripta Metallurgy Material*, 1995 (submitted).
2. Noebe, R. D., Bowman, R. R. and Nathal, M. V., Physical and mechanical properties of the B2 compound NiAl. *International Material Review*, 1993, **38**(4), 193–232.

3. Vedula, K., Pathare, V., Aslandis, I. and Titran, R., Alloys based on NiAl for high temperature applications. *Material Research Society Symposium Proceedings*, 1985, **39,** 411–421.
4. Takasugi, T., Watanabe, S. and Hanada, S., The temperature and orientation dependence of tensile deformation and fracture in NiAl single crystals. *Material Science Engineering*, 1992, **A149,** 183–193.
5. Darolia, R., NiAl alloys for high-temperature structural applications. *JOM*, 1991, 44–49.
6. Sen, S. and Stefanescu, D. M., Melting and casting processes for high-temperature intermetallics. *JOM*, 1991, 30–32.
7. Shyy, W., Udaykumar, H. S., Rao, M. M. and Smith, R. W., *Computational Fluid Dynamics with Moving Boundaries*. Taylor and Francis, Washington, D.C., 1996.
8. Ouyang, H. and Shyy, W., Multi-zone simulation of the Bridgman growth process of β-NiAl crystal. *International Journal of Heat and Mass Transfer*, 1996, **39,** 2039–2051.
9. Perry, R. H., Green, D. W. and Maloney, J. O., *Perry's Chemical Engineerings' Handbook*, 6th edn. McGraw-Hill, New York, 1984.
10. Walston, W. S. and Darolia, R., Effect of alloying on physical properties of NiAl. *MRS Symposium Proceedings*, 1995, **28,** 237–242.
11. Sen, S., Konkel, W. H., Tighe, S. J., Bland, L. G., Sharma, S. R. and Taylor, R. E., Crystal growth of large-area single-crystal CdTe and CdZnTe by the computer-controlled vertical modified-Bridgman process. *Journal Crystal Growth*, 1988, **86,** 111–117.
12. Brown, R. A., Theory of transport processes in single crystal growth from the melt. *A.I.Ch.E. Journal*, 1988, **34,** 881–911.
13. Kurz, W. and Fisher, D. J., *Fundamentals of Solidification*. Trans Tech Publications Ltd, Switzerland, 1989.